Mem. Fac. Eng., Kyoto Univ. Vol. 54, No. 4 (1992)

Epitaxial Growth of β-SiC on α-SiC Substrates by Chemical Vapor Deposition

by

Katsushi NISHINO*, Tsunenobu KIMOTO*, and Hiroyuki MATSUNAMI*

(Received June 24, 1992)

Abstract

Epitaxial growth of crystalline silicon carbide (SiC) on α-SiC substrates was carried out by chemical vapor deposition. β-SiC (3C-SiC) (111) can be epitaxially grown on a 15R-SiC (0001) substrate. The grown layers have far fewer DPBs (double positioning boundaries) than those on a 6H-SiC substrate. Successive etching of the grown layer revealed that the DPBs decreased as crystal growth proceeded. The decrease in DPBs was analyzed semi-quantitatively based on a model proposed by the authors, and the disappearance of DPBs was predicted. Schottky barrier diodes were fabricated on the grown layer and the electrical properties were investigated. The diode has a high breakdown voltage of 300V.

1. Introduction

Silicon carbide (SiC) is an attractive wide-gap semiconductor and a candidate for high-power, high-temperature and radiation-damage-resistant devices. Polytypism in SiC is well known. Cubic-SiC (3C-SiC) is called β-SiC and others (4H-, 6H-, 15R-SiC etc.) α-SiC. 3C-SiC has many attractive properties such as large band gap (2.2eV at room temperature),[1] high electron mobility ($1000 cm^2/V \cdot s$),[2] and high electron saturation drift velocity ($2.7 \times 10^7 cm/s$).[3]

Epitaxial growth of 3C-SiC has been mainly carried out on Si substrates, and 3C-SiC with a large area can be obtained. By the introduction of a buffer layer (carbonized layer), relatively high-quality 3C-SiC films can be obtained.[4,5] Fabrication of devices such as MOSFETs (metal-oxide-semiconductor field-effect transistors), MESFETs (metal-semiconductor FETs), and HBTs (heterojunction bipolar transistors) using 3C-SiC on Si has been reported.[6-8] But a large lattice mismatch of 20% and a difference in thermal expansion coefficient of 8% exist between 3C-SiC and Si, and the grown layer has a high density of defects such as misfit dislocations and stacking faults. 6H-SiC, which has very little lattice mismatch with 3C-SiC, has been also used as a substrate, and it was reported that the layers grown on 6H-SiC had a much lower density of defects than that on Si.[9] Fabrication

* Dept. of Electrical Engineering, II

of MOSFETs using 3C-SiC on 6H-SiC was reported.[6] However, the grown layers have double positioning twinning which has two domains rotated by 180° with each other along ⟨111⟩ axis, and the layers show many DPBs (double positioning boundaries)[9] on the surface. A schematic cross-sectional view of a DPB and the stacking sequence in the adjacent domains are shown in Fig. 1 (b). Here, A, B and C denote the position of Si-C pair in hexagonal close packing (Fig. 1 (a)).

Recently, the possibility of DPB-free 3C-SiC growth on 15R-SiC was suggested by Yoo based on the electrostatic model.[10] Figure 2 shows the stacking sequence of 6H-SiC and 15R-SiC. In the case of 6H-SiC, ABC... stacking is composed of three sites; from first A site to B, C and second A site. ACB... stacking is also composed of three sites; from second A site to C, B and third A site. Therefore, the ratio of ABC... stacking to ACB...

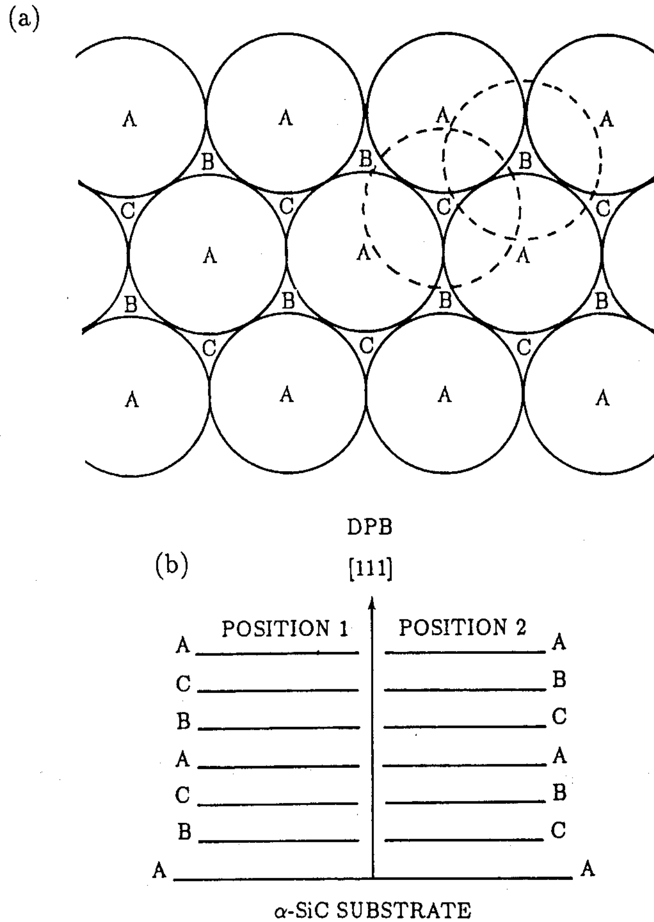

Fig. 1 Schematics of explanation for the formation of DPBs. (a) Close packing of equal spheres. (b) Model for DPB.

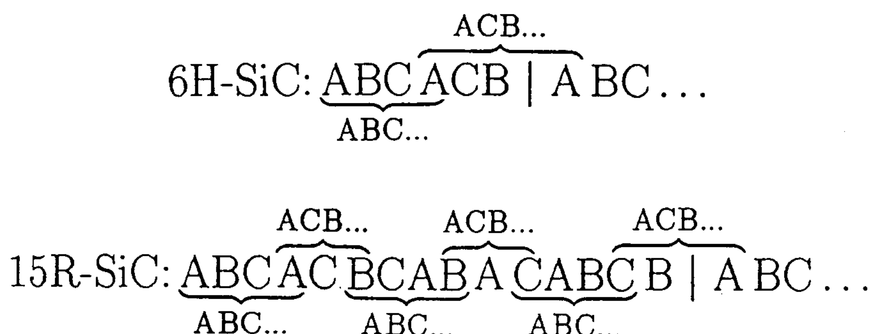

Fig. 2 The stacking sequence of 6H-SiC and 15R-SiC.

stacking is 1 : 1. Similarly, in 15R-SiC, ABC... stacking is composed of three sites, whereas ACB... stacking is composed of two sites; from second A site to C and B. Therefore, the ratio is 3 : 2. These ratios appear as the area ratio of ABC... domain to ACB... domain for the surface of a substrate. According to the model, the area ratio of the two domains on the substrate surface affects that of the two domains in the grown layer at the initial stage of growth. The area ratio of domains becomes larger with growth, and the disappearance of DPBs is expected.

In this paper, epitaxial growth of 3C-SiC on 15R-SiC substrates, analysis of decrease in DPBs and the electrical properties of grown layers are described.

2. Experiments

A schematic diagram of the growth system is shown in Fig. 3. A horizontal quartz reaction tube with a water-cooling jacket was used. A substrate was heated by rf induction. H_2 gas refined by a purifier was used as a carrier gas, and source gases were SiH_4 and C_3H_8.

As substrates, 6H-SiC and 15R-SiC natural {0001} faces produced by the Acheson process were used. The (0001) Si face or $(000\bar{1})$ C face of a substrate was distinguished by the difference in the thickness of the resultant oxide layer. The C face is more reactive, causing it to be oxidized faster than the Si face. So, a cleaved piece of a substrate was oxidized in a dry O_2 atmosphere at 1100°C for 5 hours, and the face was identified. Prior to growth, substrates were cleaned in organic solvent, HCl, *aqua regia* ($HCl : HNO_3 = 3 : 1$), HF, and deionized water. Oxidation or polishing of substrates was not performed.

Growth was carried out under atmospheric pressure. The growth temperature was 1500°C, which was monitored by a pyrometer. The growth procedure was as follows:

1. The temperature was increased to 1500°C in a hydrogen atmosphere.
2. The source gases were introduced.

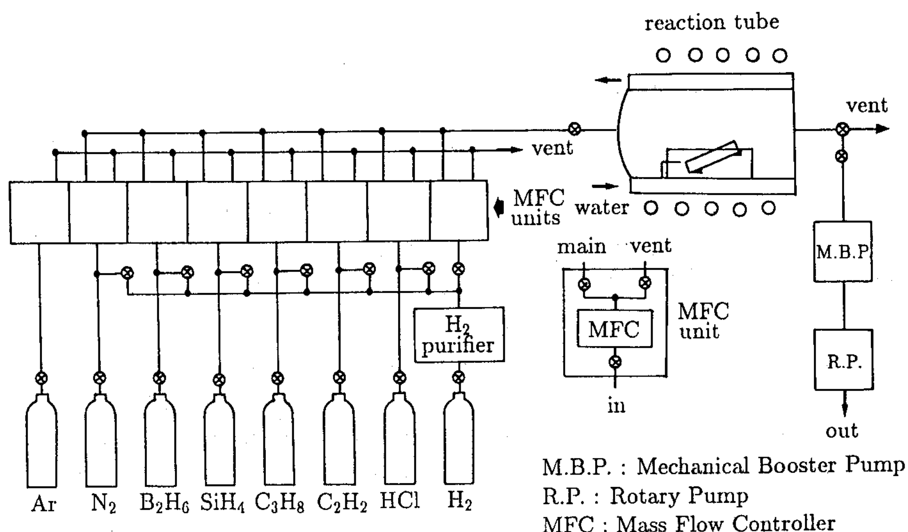

Fig. 3 A schematic diagram of the growth system.

3. Crystal growth.
4. After the desired time, the source gases were stopped.
5. The rf power was turned off.

The polytype of grown layers was identified by RHEED (Reflection High-Energy Electron Diffraction), etch-pit observation with molten KOH, and photoluminescence. Photoluminescence was measured at 14 K by excitation with a He-Cd laser (wavelength: 325 nm).

Successive etching was carried out as follows:

1. Polishing the surface ($1 \sim 2\,\mu$m) with diamond paste.
2. Etching the surface with molten KOH at 500°C so that DPBs can be observed.
3. Surface observation.

This process was repeated.

Au was evaporated in a vacuum ($\sim 10^{-6}$ Torr) as Schottky contacts and Au : Ta (99 : 1) as ohmic contacts. Prior to evaporation, samples were cleaned in organic solvent, HCl, deionized water and a 20% hot solution (95°C) of K_2CO_3. Cleaning in this hot solution was confirmed to be effective for the improvement of current-voltage characteristics of Schottky barriers.[11]

3. Results and Discussion

3.1 Epitaxial growth on α-SiC substrates

Crystal growth on α-SiC substrates was carried out by atmospheric chemical vapor

deposition. The substrates were 6H-SiC and 15R-SiC Si faces. The typical flow rates of H_2, SiH_4, and C_3H_8 were 3 slm, 0.30 sccm, and 0.20 sccm, respectively. In this case, the growth rate is 2.5 μm/h. Typical growth time is 2 hours. Nomarski microphotographs of the surface for the grown layers are shown in Fig 4. Mosaic patterns corresponding to DPBs were observed for the layer grown on 6H-SiC. Although small mosaic patterns are also observed for the layer grown on 15R-SiC, the layer has far fewer DPBs than that on 6H-SiC. When a 15R-SiC C face was used as a substrate, the grown layer had a very rough surface. The following results and discussion are only for Si face substrates.

Figure 5 shows the photoluminescence spectrum of the layer grown on 15R-SiC for 6

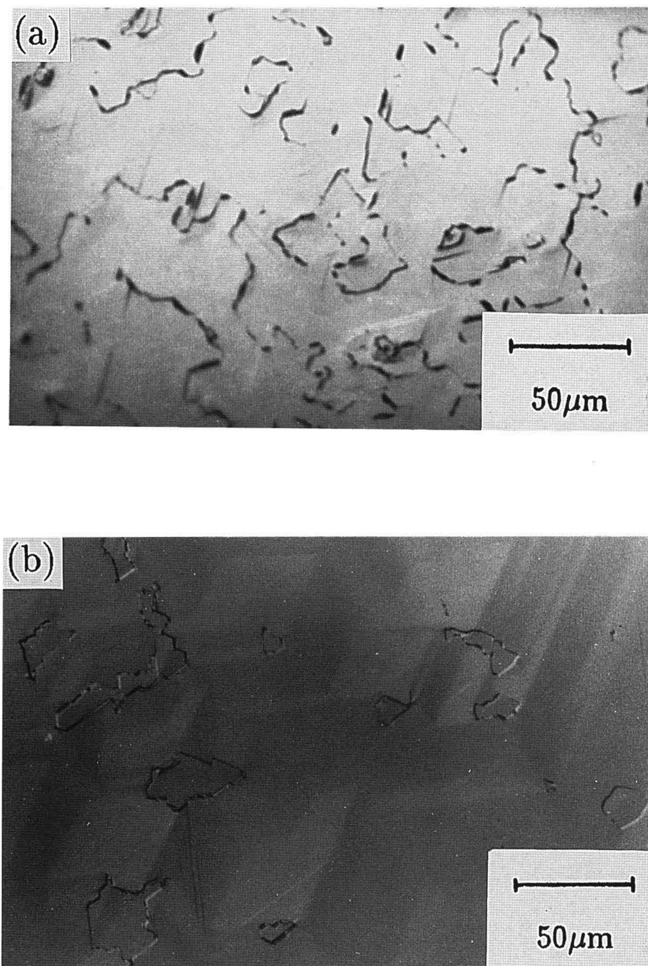

Fig. 4 Nomarski microphotographs of the grown layers (a) on 6H-SiC (0001), and (b) on 15R-SiC (0001).

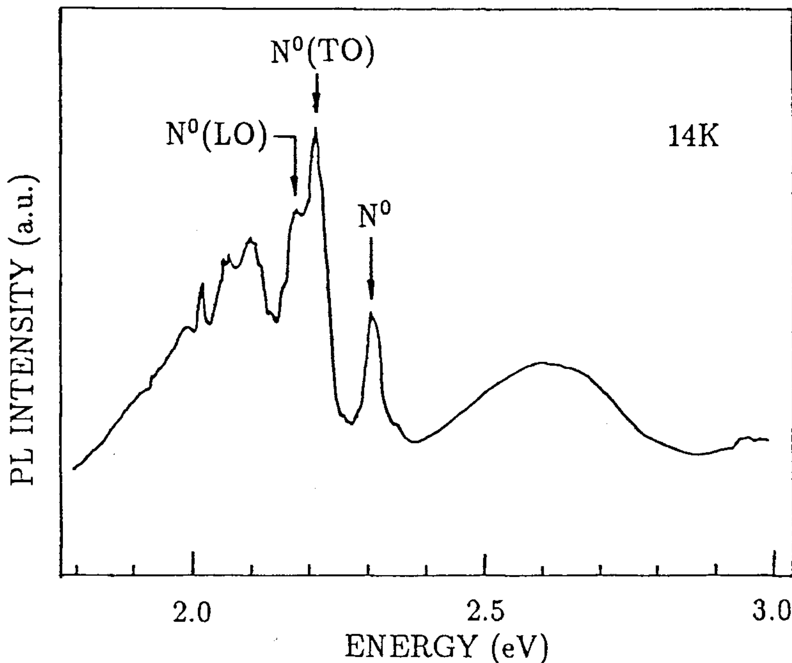

Fig. 5 A photoluminescence spectrum of the grown layer at 14K.

hours. The luminescence peaks were observed at 2.31, 2.22, and 2.18 eV, and these peaks agree with the nitrogen-bound exciton line (N^0), its transverse optical phonon replica (N^0(TO)) and longitudinal optical phonon replica (N^0(LO)) of 3C-SiC, respectively.[12] Any other peaks for α-SiC at about 3 eV were not observed. Then, the grown layer was identified as 3C-SiC.

Figure 6(a) shows the RHEED pattern of the grown layer*. Figure 6(b) shows the theoretical ⟨110⟩-azimuth RHEED pattern of 3C-SiC (111) containing twinning (double positioning). White circles represent diffraction spots from single crystalline 3C-SiC (111) (ABC... stacking) domains, and black circles that from 3C-SiC (111) (ACB... stacking) domains. The white circles with black dots are common diffraction spots for the two kinds of 3C-SiC (ABC... and ACB... stackings). Thus, the grown layer was identified as 3C-SiC by RHEED analysis. For the layer grown on 6H-SiC, the observed intensity of the spots corresponding to ABC... domain and that to ACB... domain are almost equal. For the layer grown on 15R-SiC, much stronger spots corresponding to ABC... domains were observed. Since the area irradiated with an electron beam in RHEED analysis is estimated

* Prior to RHEED analysis, samples were etched with molten KOH at 600°C for 10 sec to make the surface rough, which gives spot patterns in RHEED.

to be $0.1 \times 10\,mm^2$, the ratio of the diffraction intensities corresponds to the area ratio of the two domains. The layer grown on 15R-SiC is almost single domain 3C-SiC (111) (ABC... stacking).

Figure 7 shows the SEM (scanning electron microscope) image of the etched surface of the grown layer. Etching was carried out with molten KOH at 500°C for 30 sec. Triangular pits were observed. It is known that 3C-SiC shows triangular pits,

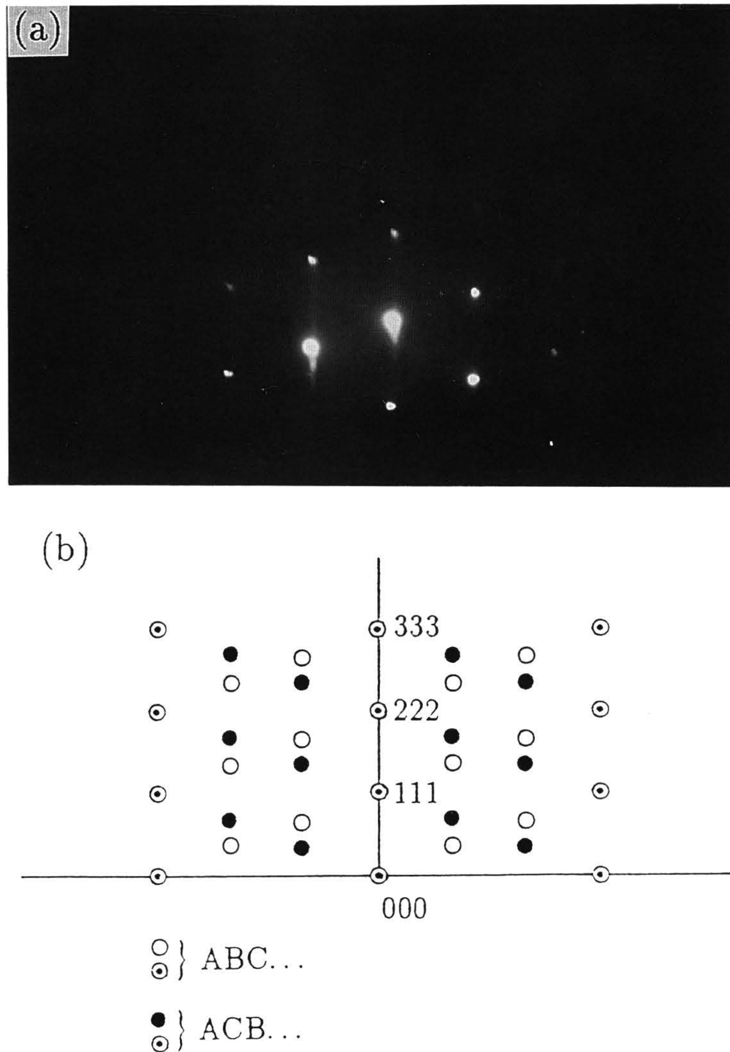

Fig. 6 (a) Observed RHEED pattern of the layer grown on 15R-SiC.
(b) Theoretical ⟨110⟩-azimuth RHEED pattern of 3C-SiC (111) containing twining (double positioning).

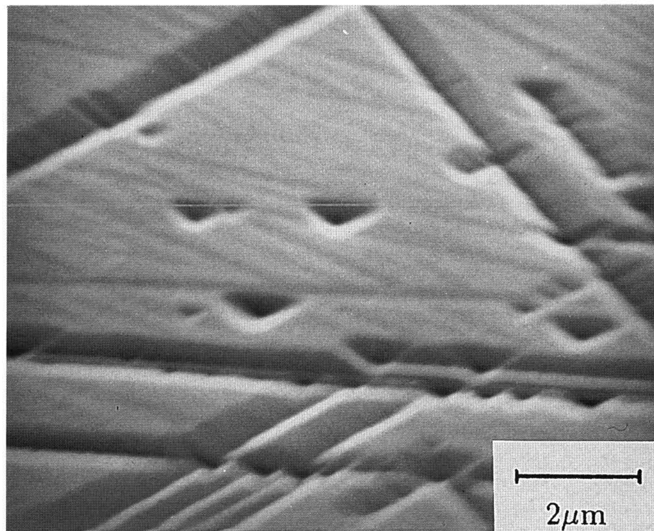

Fig. 7 SEM image of etched surface of the grown layer with molten KOH.

6H- and 4H-SiC show hexagonal pits, and 15R-SiC shows distorted hexagonal pits.[13,14] The grown layer was also identified as 3C-SiC by etch-pit observation. The straight lines intersecting at 60° with each other correspond to stacking faults.

3.2 The decrease in DPBs

A grown layer with a thickness of about 30 μm was etched successively and the decrease in DPBs was investigated. An example of microphotographs of the etched surfaces is shown in Fig. 8. The ratio of the sum of each DPB area** to the whole area against layer thickness is shown in Fig. 9 with white circles. The layer thickness dependence of each DPB area is also shown in Fig. 9 as black circles and squares. The curves in the figure will be discussed below. The ratio decreases monotonically with the thickness of grown layers, and each DPB area decreases similarly.

Figures 10(a) and (b) show typical small DPBs. Their forms are triangular or hexagonal. Most of the other small DPBs have similar forms, and DPBs are thought to decrease anisotropically.

On the basis of these results, a model for the decrease in DPBs is proposed. It is assumed that an initial DPB form is a circle with radius r and that it goes inward anisotropically from three or six directions with velocity v (Fig. 11). From this model, DPB area S can be expressed in the following equations as functions of growth time t (see appendix).

** DPB area is defined as the area surrounded by DPB.

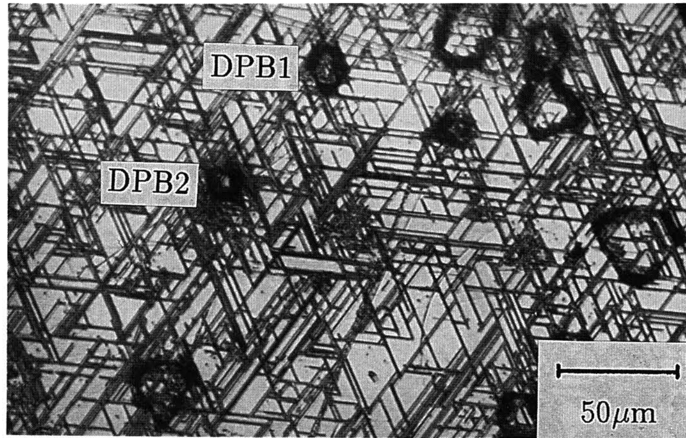

Fig. 8 An example of microphotograph for etched surfaces.

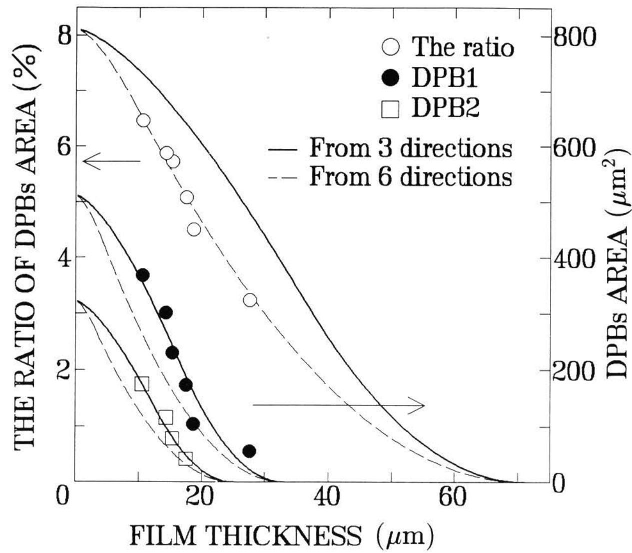

Fig. 9 Film thickness dependence of the ratio of DPBs area to the whole area and of each DPB area.

When a DPB decreases from three directions:

$$S = \begin{cases} \pi r^2 + \dfrac{3}{2} r^2 (\sin\theta - \theta) & \left(0 \le vt \le \dfrac{1}{2} r\right), \\ 3\sqrt{3}(r - vt)^2 & \left(\dfrac{1}{2} r \le vt \le r\right). \end{cases} \tag{1}$$

When a DPB decreases from six directions:

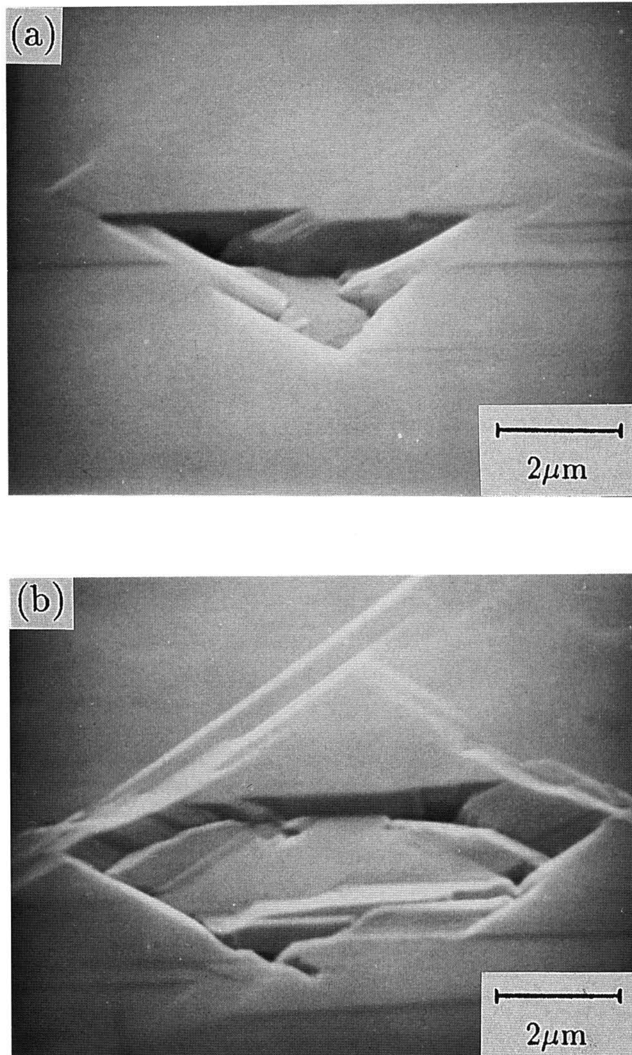

Fig. 10 SEM images of small DPBs in forms of (a) triangle or (b) hexagon.

$$S = \begin{cases} \pi r^2 + 3r^2(\sin\theta - \theta) & \left(0 \le vt \le \left(1 - \dfrac{\sqrt{3}}{2}\right)r\right), \\ 2\sqrt{3}(r - vt)^2 & \left(\left(1 - \dfrac{\sqrt{3}}{2}\right)r \le vt \le r\right), \end{cases} \tag{2}$$

where $\theta = 2 \arccos\left(1 - \dfrac{vt}{r}\right)$.

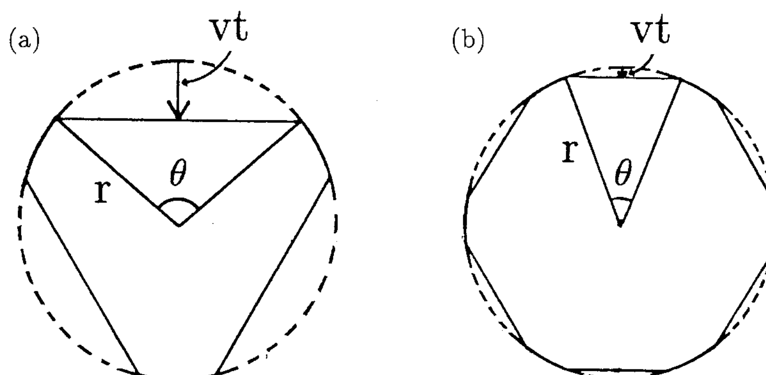

Fig. 11 A model for the decrease in DPBs. An initial DPB form is a circle of radius r, and it goes inward anisotropically from (a) three directions or (b) six directions with velocity v.

We tried to fit this model to the experimental results. In fitting, film thickness was used instead of growth time because film thickness is thought to be proportional to growth time. The data for the ratio of the sum of each DPB area to the whole area fit the model that a DPB decreases from six directions (Fig. 9). In this case, r is given as $32\,\mu m$ and v as $0.45\,\mu m$ per $1\,\mu m$ of film thickness. DPBs are expected to disappear at a film thickness of $71\,\mu m$. So, DPB-free 3C-SiC might be obtained if the thickness of the grown layer increases up to several ten microns. The data for each DPB area fit the model that a DPB decreases from three directions (Fig. 9). In the case of DPB1, r is given as $13\,\mu m$ and v as $0.39\,\mu m$ per $1\,\mu m$ of film thickness. In the case of DPB2, r is given as $10\,\mu m$ and v as $0.40\,\mu m$ per $1\,\mu m$ of film thickness.

Thus, the sum of each DPB area fits the model that a DPB decreases from six directions, and each DPB area fits the model of decreasing from three directions. These results may be explained as follows. Although it is assumed that a DPB decreases inward from six directions in equal velocity, the six directions may not be equivalent. They may have three fast-decreasing directions and three slow-decreasing directions: initially the form of a DPB is hexagonal, and it gradually becomes triangular. The contribution of large DPBs to the sum of each DPB area is larger than that of small DPBs, and so, the decrease in the sum of each DPB area fits the model of decreasing from six directions. The thickness at which the fitted model changes from six directions to three directions may depend on a DPB form in the initial stage of growth.

The obtained value of v is considered to be related to the mechanism of the decrease in DPBs. To reveal the mechanism, further experiments such as TEM (transmission electron microscope) observation are necessary.

3.3 Electrical properties

Schottky barrier diodes were fabricated and the electrical properties of the grown layers were investigated. Both Schottky contacts and ohmic contacts were evaporated on the surface of the grown layer. The area of each Schottky contact was $7.07 \times 10^{-4}\,cm^2$.

An example of current-voltage (I-V) characteristics is shown in Fig. 12. Although

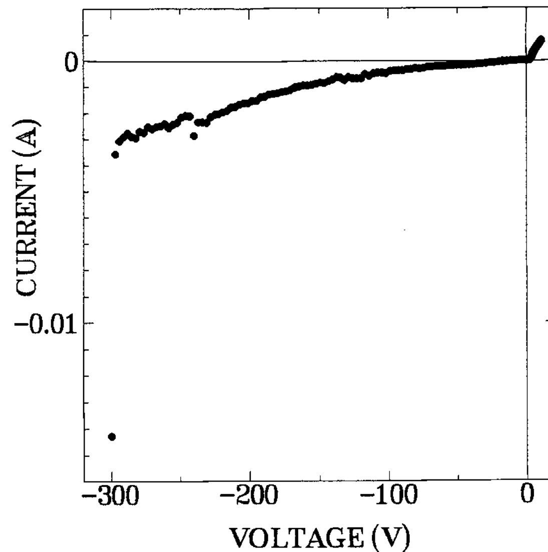

Fig. 12 I-V characteristics of a Schottky barrier diode.

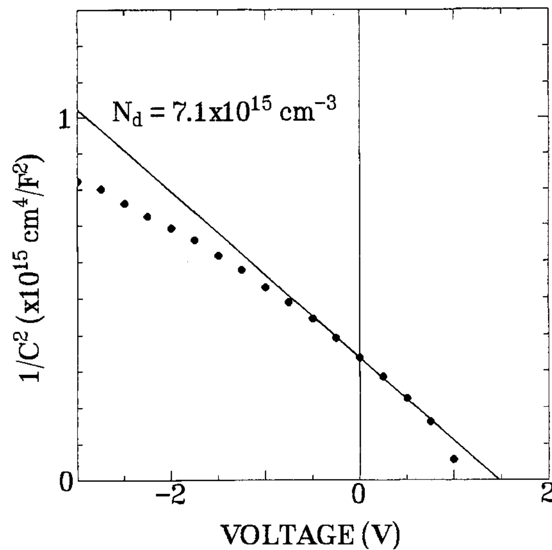

Fig. 13 $1/C^2$-V characteristics of the Schottky barrier diode.

leakage current is relatively large, the diode showed "hard" breakdown, and the breakdown voltage obtained was 300 V. This is the highest value of those which have been reported on 3C-SiC.

Capacitance-voltage ($1/C^2$-V) characteristics of the diode are shown in Fig. 13. Donor concentration N_d determined from the characteristics was $7.1 \times 10^{15}\,\mathrm{cm}^{-3}$.

4. Conclusion

Epitaxial growth of 3C-SiC (111) with far fewer DPBs could be achieved by the use of 15R-SiC (0001) as a substrate. DPBs were decreased monotonically with the increase in film thickness. A model for the decrease in DPBs was proposed. On the basis of the model, the velocity of the decrease in DPBs was obtained, and the layer thickness for the disappearance of DPBs was predicted. Schottky barrier diodes were fabricated on the grown layer. The diode had the highest breakdown voltage (300 V) of those which have been reported on 3C-SiC.

Appendix

The derivation of the equations in the model for decrease in DPB

First, consider the model that a DPB decreases from three directions. A circle with radius r is divided into three equal fan-shaped areas as shown in Fig. A1 (a). One area S_1 can be expressed as the sum of the triangle and the fan-shaped area, and is described in the following equation,

$$S_1 = \frac{1}{2}r^2 \sin\theta + \frac{1}{2}r^2\left(\frac{2\pi}{3} - \theta\right), \tag{A1}$$

where v is the velocity for DPB to decrease inward and t is growth time. DPB area S is three times S_1, and so,

$$\begin{aligned} S = 3S_1 &= 3\left\{\frac{1}{2}r^2 \sin\theta + \frac{1}{2}r^2\left(\frac{2\pi}{3} - \theta\right)\right\} \\ &= \pi r^2 + \frac{3}{2}r^2(\sin\theta - \theta). \end{aligned} \tag{A2}$$

Similarly, in the case of the model that a DPB decreases from six directions as shown in Fig. A1 (b), DPB area S is expressed in the following equation,

$$\begin{aligned} S &= 6\left\{\frac{1}{2}r^2 \sin\theta + \frac{1}{2}r^2\left(\frac{\pi}{3} - \theta\right)\right\} \\ &= \pi r^2 + 3r^2(\sin\theta - \theta). \end{aligned} \tag{A3}$$

In each case, it is satisfied that $r\cos(\theta/2) = r - vt$ or $\theta = 2\arccos\left(1 - \frac{vt}{r}\right)$.

In the case of DPB decreasing from three directions, DPB becomes triangular when $\theta = 2\pi/3$ or $vt = r/2$, and DPB area is

$$S = 3\sqrt{3}(r - vt)^2. \tag{A4}$$

Similarly, in the case of DPB decreasing from six directions, after $\theta = \pi/3$ or $vt = \left(1 - \frac{\sqrt{3}}{2}\right)r$, DPB area is

$$S = 2\sqrt{3}(r - vt)^2. \tag{A5}$$

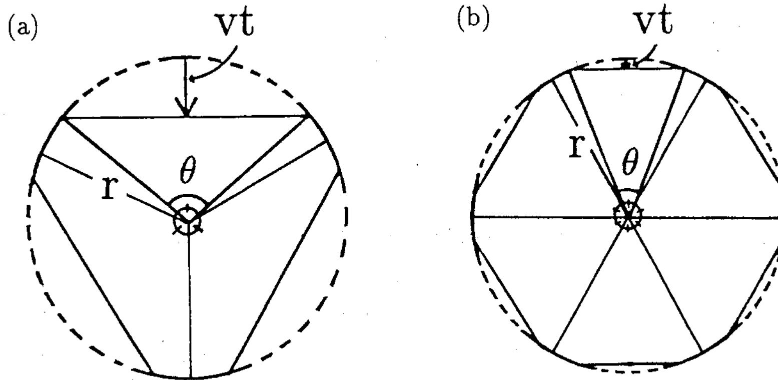

Fig. A1 A model that a DPB decrease (a) from three directions, and (b) from six directions.

References

1) H. R. Philipp and E. A. Taft, Silicon Carbide (Pergamon Press 1960) p. 366.
2) W. E. Nelson, F. A. Halden, and A. Rosengreen, J. Appl. Phys., **37** 353 (1966).
3) D. K. Ferry, Phys. Rev., **B12** 2361 (1975).
4) H. Matsunami, S. Nishino, and H. Ono, IEEE Trans. Electron Devices, **ED-28** 1235 (1981).
5) S. Nishino, H. Suhara, and H. Matsunami, Extended Abst. 15th Conf. SSDM, Tokyo p. 317 (1983).
6) J. W. Palmour, H. S. Kong, and R. F. Davis, J. Appl. Phys., **64** 2168 (1988).
7) H. Daimon, M. Yamanaka, M. Shinohara, E. Sakuma, S. Misawa, K. Endo, and S. Yoshida, Appl. Phys. Lett., **51** 2106 (1987).
8) T. Sugii, T. Ito, Y. Furumura, M. Doki, F. Mieno, and M. Maeda, IEEE Electron Device Letters, **9** 87 (1988).
9) H. S. Kong, B. L. Jiang, J. T. Glass, G. A. Rozgonyi, and K. L. More, J. Appl. Phys., **63** 2645 (1988).
10) W. S. Yoo et al., Extended Abstracts of 4th Intern. Conf. on Amorphous and Crystalline Silicon

Carbide and other IV-IV Materials (ICACSC '91), I.8.
11) H. Suhara, Master Thesis, Faculty of Engineering, Kyoto University, 1983.
12) W. J. Choyke, Z. C. Feng, and J. A. Powell, J. Appl. Phys., **64** 3163 (1988).
13) *Silicon Carbide-1973* edited by R. C. Marshall, J. W. Faust, Jr., and C. E. Ryan, (University of South Carolina Press Columbia, S. C., 1974) p. 215.
14) J. W. Faust, Jr., Silicon Carbide (Pergamon Press 1960) p. 403.